

A possible evidence of observation of two mixed phases in nuclear collisions

K.A. Bugaev¹, A.I. Ivanytskyi¹, V.V. Sagun¹, G.M. Zinovjev¹, D.R. Oliinychenko^{1,2}, V.S. Trubnikov³, and E.G. Nikonov⁴

¹ *Bogolyubov Institute for Theoretical Physics of the National Academy of Sciences of Ukraine, 03680, Kiev, Ukraine*

² *FIAS, Goethe University, Ruth-Moufang Str. 1, 60438 Frankfurt upon Main, Germany*

³ *National Science Center "Kharkov Institute of Physics and Technology", 61108, Kharkov, Ukraine*

⁴ *Laboratory for Information Technologies, JINR, Joliot-Curie Str. 6, Dubna 141980, Russia*

Abstract. Using an advanced version of the hadron resonance gas model we have found several remarkable irregularities at chemical freeze-out. The most prominent of them are two sets of highly correlated quasi-plateaus in the collision energy dependence of the entropy per baryon, total pion number per baryon, and thermal pion number per baryon which we found at center of mass energies 3.6-4.9 GeV and 7.6-10 GeV. The low energy set of quasi-plateaus was predicted a long time ago. On the basis of the generalized shock-adiabat model we demonstrate that the low energy correlated quasi-plateaus give evidence for the anomalous thermodynamic properties of the mixed phase at its boundary to the quark-gluon plasma. The question is whether the high energy correlated quasi-plateaus are also related to some kind of mixed phase. In order to answer this question we employ the results of a systematic meta-analysis of the quality of data description of 10 existing event generators of nucleus-nucleus collisions in the range of center of mass collision energies from 3.1 GeV to 17.3 GeV. These generators are divided into two groups: the first group includes the generators which account for the quark-gluon plasma formation during nuclear collisions, while the second group includes the generators which do not assume the quark-gluon plasma formation in such collisions. Comparing the quality of data description of more than a hundred of different data sets of strange hadrons by these two groups of generators, we find two regions of the equal quality of data description which are located at the center of mass collision energies 4.3-4.9 GeV and 10.-13.5 GeV. These two regions of equal quality of data description we interpret as regions of the hadron-quark-gluon mixed phase formation. Such a conclusion is strongly supported by the irregularities in the collision energy dependence of the experimental ratios of the Lambda hyperon number per proton and positive kaon number per Lambda hyperon. Although at the moment it is unclear, whether these regions belong to the same mixed phase or not, there are arguments that the most probable collision energy range to probe the QCD phase diagram (tri)critical endpoint is 12-14 GeV.

1 Introduction

The hadron resonance gas model (HRGM) [1] is traditionally used to extract the parameters of chemical freeze-out (CFO) from the measured hadronic yields. Its version with the multicomponent hard-

core repulsion [2–4] allowed one for the first time to successfully describe the most problematic ratios K^+/π^+ with $\chi^2/dof = 3.9/14$ and Λ/π^- with $\chi^2/dof = 10.2/12$ without spoiling all other hadron yield ratios [5, 6]. Fig. 1 demonstrates the present fit quality of these traditionally problematic ratios. The achieved high quality $\chi^2/dof \approx 0.95$ [5, 6] of data description of 111 independent hadron yield ratios measured at midrapidity in central nucleus-nucleus collisions at the center of mass energies $\sqrt{s_{NN}} = 2.7, 3.1, 3.6, 4.3, 4.9, 6.3, 7.6, 8.8, 9.2, 12.3, 17.3, 62.4, 130, 200$ GeV proves that the multi-component version of HRGM is a precise and a sensitive tool of heavy ion collision phenomenology.

Using the multicomponent version of HRGM it was possible to reveal a few novel irregularities at CFO. The most remarkable of them are two sets of highly correlated quasi-plateaus in the collision energy dependence of the entropy per baryon, total pion number per baryon, and thermal pion number per baryon which were found at the center of mass energies 3.6–4.9 GeV and 7.6–10 GeV [7] and the sharp peak of the trace anomaly found at the center of mass energy 4.9 GeV [8]. The low energy set of quasi-plateaus was predicted a long time ago [9–11] as a signal of the anomalous thermodynamic properties inside the quark-gluon-hadron mixed phase. Unfortunately, the generalized shock-adiabat model cannot be safely applied to the central nuclear collisions at $\sqrt{s_{NN}} \geq 7.6$ GeV [9]. Therefore, in order to correctly interpret the high energy quasi-plateaus here we use the results of meta-analysis [12] of the quality of data description (QDD) of 10 existing event generators of nucleus-nucleus collisions along with the thorough analysis of irregularities in the existing experimental hadron yield ratios.

The work is organized as follows. In Sect. 2 we remind the basic elements of the HRGM with multicomponent hard-core repulsion. A brief description of the meta-analysis suggested in [12] is presented in Sect. 3 along with a discussion of existing hadron multiplicity data which help to shed light on the problem of the formation of two quark-gluon-hadron mixed phases. In Sect. 4 our conclusions are formulated.

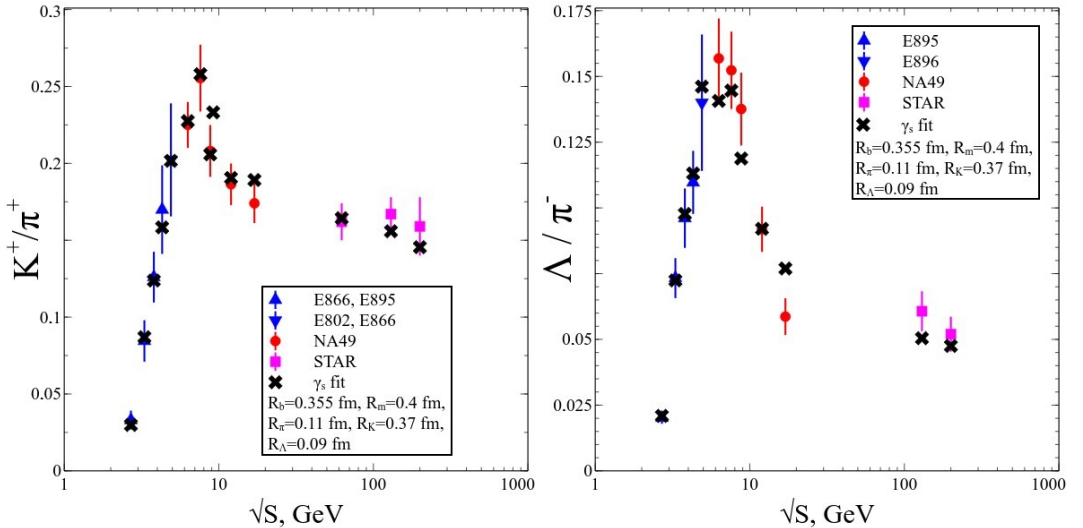


Figure 1. Collision energy dependence of K^+/π^+ and Λ/π^- hadron yield ratios which traditionally were the most problematic ones.

2 HRGM with multicomponent hard-core repulsion

The HRGM is based on the assumption of local thermal and chemical equilibrium at CFO. Hence the hadron yields produced in the collisions of large atomic nuclei can be found using the grand canonical valuables, i.e. using the temperature T , the baryonic μ_B , the strange μ_s and the isospin third projection μ_{I3} chemical potentials. As usual, the chemical potential μ_s is fixed by the condition of zero total strange charge. The possible deviation of strange charge from the full chemical equilibrium is taken into account by the parameter γ_s [13]. It changes the thermal density φ_j of hadron sort j as $\varphi_j \rightarrow \gamma_s^{S_j} \varphi_j$, where S_j is the total number of strange valence quarks and antiquarks in such a hadron.

The main difference of the present version of HRGM from the ones developed by other authors is that in our HRGM several sorts of hadrons have individual hard-core radii. Thus, it employs different hard-core radii for pions, R_π , kaons, R_K , Λ -hyperons, R_Λ , other mesons, R_m , and baryons, R_b . The best global fit of 111 independent hadronic multiplicities measured in the whole collision energy range from $\sqrt{s_{NN}} = 2.7$ GeV to $\sqrt{s_{NN}} = 200$ GeV was found for $R_b = 0.355$ fm, $R_m = 0.4$ fm, $R_\pi = 0.1$ fm, $R_K = 0.37$ fm and $R_\Lambda = 0.11$ fm with the quality $\chi^2/dof \approx 0.95$ [5, 6]. The second virial coefficient between the hadrons of hard-core radii R_i and R_j is defined as $b_{ij} = \frac{2\pi}{3}(R_i + R_j)^3$. Taking from the thermodynamic code THERMUS [14] such characteristics of hadrons of sort i as the spin-isospin degeneracy g_i , the mass m_i and the width Γ_i one can find the set of partial pressures p_i for each hadronic component ($p = \sum_i p_i$ is total pressure) from the system

$$p_i = T \varphi_i \exp \left[\frac{\mu_i - 2 \sum_j p_j b_{ji} + \sum_{jl} p_j b_{jl} p_l / p}{T} \right]. \quad (1)$$

Here $\mu_i = Q_i^B \mu_B + Q_i^{I3} \mu_{I3} + Q_i^S \mu_S$ is the full chemical potential of the i -th hadronic sort expressed via its charges $\{Q_i^A\}$ and the corresponding chemical potentials $\{\mu_A\}$ (with $A \in \{B, I3, S\}$). In the Boltzmann approximation the thermal density of i -th hadronic sort reads as

$$\varphi_i = \gamma_s^{S_i} g_i \int_{M_i}^{\infty} dm f(m, m_i, \Gamma_i) \int \frac{k^2 dk}{2\pi^2} e^{-\frac{\sqrt{m^2 + k^2}}{T}}, \quad (2)$$

where M_i is a threshold of its dominant decay channel and f is the normalized Breit-Wigner mass attenuation function. Thermal multiplicities $N_i^{th} = V \frac{\partial p}{\partial \mu_i}$ (V is the effective volume at CFO) should be corrected by the hadron decays after the CFO according to the branching ratios $Br_{l \rightarrow i}$. The latter define the probability of particle l to decay into a particle i . Hence the ratio of full multiplicities can be written as

$$\frac{N_i^{tot}}{N_j^{tot}} = \frac{p_i + \sum_{l \neq i} p_l Br_{l \rightarrow i}}{p_j + \sum_{l \neq j} p_l Br_{l \rightarrow j}}. \quad (3)$$

With the help of (3) we obtained the high quality fit of experimental hadron ratios measured at AGS for energies $\sqrt{s_{NN}} = 2.7, 3.1, 3.6, 4.3, 4.9$ GeV [15–24], at SPS energies $\sqrt{s_{NN}} = 6.3, 7.6, 8.8, 12.3, 17.3$ GeV measured by the NA49 Collaboration [25–33] and at RHIC energies $\sqrt{s_{NN}} = 9.2, 62.4, 130, 200$ GeV measured by the STAR Collaboration [34]. As described in [3, 4], from these data we constructed 111 independent ratios measured at 14 values of collision energies. The most important results are shown in Figs. 1 and 2. The left panel of Fig. 2 shows the highly correlated quasi-plateaus in the collision energy dependence of the entropy per baryon s/ρ_B , total pion number per baryon ρ_π^{tot}/ρ_B , and thermal pion number per baryon ρ_π^{th}/ρ_B at laboratory energies 6.9–11.6 GeV (i.e. $\sqrt{s_{NN}} = 3.6 - 4.9$ GeV) which were found in [7]. As one can see from the left panel of Fig. 2, a clear plateau is demonstrated by the thermal pion number per baryon while other quantities show quasi-plateaus.

Nevertheless, all these quasi-plateaus are important, since their strong correlation with the plateau in the thermal pion number per baryon allows one to find out their common width in the collision energy [7, 8].

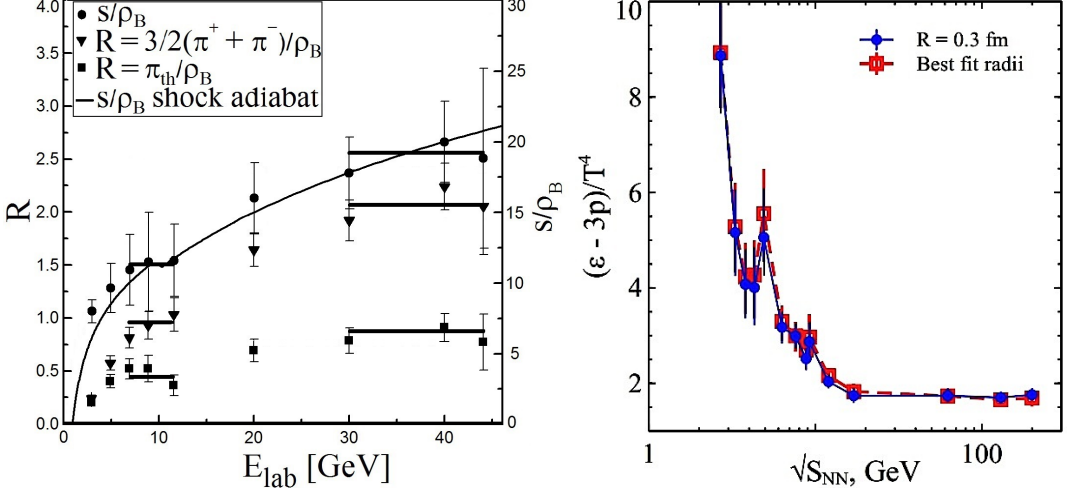


Figure 2. Left: The correlated quasi-plateaus at CFO found in [7] (see details in the text). Right: Trace anomaly as function of collision energy at CFO established in [8].

Note that these low energy quasi-plateaus were predicted about 25 years ago [9–11] as a manifestation of the anomalous thermodynamic properties of quark-gluon-hadron mixed phase. In contrast to the normal thermodynamic properties, in the medium with the anomalous ones the adiabatic compressibility of matter increases for increasing pressure. In the normal media (pure gaseous or liquid phases) there exists a repulsion between the constituents at short distances which leads to an opposite behavior of the adiabatic compressibility. Therefore, an appearance of these quasi-plateaus is a signal of the quark-gluon-hadron mixed phase formation [9–11]. Such a conclusion is strongly supported by an existence of the sharp peak of the trace anomaly $\delta = \frac{\varepsilon - 3p}{T^4}$ (here ε is energy density) at $\sqrt{s_{NN}} = 4.9$ GeV [8] (see the right panel of Fig. 2). This peak is important, since in lattice QCD an inflection or a maximum point of the trace anomaly is used for a determination of the pseudo-critical temperature of the cross-over transition [35]. One may think that a sharp peak of δ at CFO is exclusively generated by the peak of baryonic density which in our HRGM also exists at $\sqrt{s_{NN}} = 4.9$ GeV. However, the real situation is more complicated. Writing the trace anomaly as

$$\delta = \frac{\varepsilon - 3p}{T^4} = \frac{Ts + \mu_B \rho_B + \mu_{I3} \rho_{I3} - 4p}{T^4} \simeq \frac{s}{T^3} \left(1 + \frac{\mu_B \rho_B}{T s} \right) - 4 \frac{p}{T^4}, \quad (4)$$

where in the last step the small contribution $\mu_{I3} \rho_{I3}$ related to the charge of the third isospin projection is neglected. From (4) one can easily conclude that the strong increase of δ on the collision energy interval $\sqrt{s_{NN}} = [4.3; 4.9]$ GeV is provided by a strong jump of the effective number of degrees of freedom s/T^3 on this interval [8, 36]. Note that despite the existence of a baryon density peak on this interval of collision energy, the entropy per baryon s/ρ_B is constant on it as one can see from the left panel of Fig. 2. Now it is evident that without a strong jump of the effective number of degrees of freedom s/T^3 the sharp peak of trace anomaly at CFO would not exist. At higher collision energies the trace anomaly δ decreases mainly because the ratio μ_B/T strongly decreases, while the inverse

entropy per baryon decreases slowly. It is important to mention that the sharp peak of δ is seen, if the finite width of all hadronic resonances is included into the HRGM [36], while for the HRGM with a zero width of hadron resonances such a peak is washed out.

The physical origin of the trace anomaly sharp peak (and, hence, of a strong jump of the effective number of degrees of freedom s/T^3) at CFO found at $\sqrt{s_{NN}} = 4.9$ GeV is rooted in the trace anomaly peak existing at the shock adiabat [8]. The shock adiabat model reasonably well describes the hydrodynamic and thermodynamic quantities of the initial state formed in the central nucleus-nucleus collisions in the laboratory energy range $1 \text{ GeV} \leq E_{lab} \leq 30 \text{ GeV}$ [8], while at higher collision energies, i.e. for $\sqrt{s_{NN}} \geq 7.6$ GeV, it can be used for qualitative estimates. In [8] it was found that the peak of δ at the shock adiabat appears at the collision energy corresponding exactly to the boundary between the quark gluon plasma (QGP) and quark-gluon-hadron mixed phase and, therefore, the trace anomaly sharp peak at CFO is a signal of QGP formation. In this respect it is interesting that in the right panel of Fig. 2 one can see a second peak of trace anomaly located at $\sqrt{s_{NN}} = 9.2$ GeV. Although the second peak of δ is less pronounced than the first one, it is also associated to the high energy set of quasi-plateaus shown in the left panel of Fig. 2 at the collision energy interval $E_{lab} = [30; 44.]$ GeV ($\sqrt{s_{NN}} = [7.6; 9.2]$ GeV). Therefore, the future experiments at RHIC, NICA and FAIR will have to find out whether the high energy peak of trace anomaly has any physical meaning.

3 Meta-analysis of quality of data description

The main objects of a meta-analysis suggested in [12] are the mean deviation squared of the quantity $A^{model,h}$ of the model M from the data $A^{data,h}$ per number of the data points n_d for a particle type h

$$\langle \chi^2/n \rangle_A^h \Big|_M = \frac{1}{n_d} \sum_{k=1}^{n_d} \left[\frac{A_k^{data,h} - A_k^{model,h}}{\delta A_k^{data,h}} \right]^2 \Big|_M, \quad (5)$$

and its error which is defined according to the rule of indirect measurements [58] as

$$\Delta_A \langle \chi^2/n \rangle_A^h \Big|_M \equiv \left[\sum_{k=1}^{n_d} \left[\delta A_k^{data,h} \frac{\partial \langle \chi^2/n \rangle_A^h \Big|_M}{\partial A_k^{data,h}} \right]^2 \right]^{\frac{1}{2}} \equiv \frac{2}{\sqrt{n_d}} \sqrt{\langle \chi^2/n \rangle_A^h \Big|_M}, \quad (6)$$

where $\delta A_k^{data,h}$ is an experimental error of the experimental quantity $A_k^{data,h}$ and the summation in Eqs. (5) and (6) runs over all data point n_d at given collision energy. For a convenience the quantity defined in (5) is called the quality of data description (QDD). To get the most complete picture of the dynamics of nuclear collisions, one has to compare the available data on the transverse mass (m_T) distributions $A = \frac{1}{m_T} \frac{d^2 N(m_T, y)}{dm_T dy}$, the longitudinal rapidity (y) distributions $A = \frac{dN(y)}{dy}$ and the hadronic yields (Y) measured at midrapidity $A = \frac{dN(y=0)}{dy}$ or/and the total one, i.e. measured within 4π solid angle, since right these observables are traditionally believed to be sensitive to the equation of state properties [37, 38].

The QDD of strange hadrons was found for two types of models [12]:

- **The hadron gas (HG) models** are as follows: ARC [39], RQMD2.1(2.3) [40], HSD [41–43], UrQMD1.3(2.0, 2.1, 2.3) [44], statistical hadronization model (SHM) [45] and AGSHJET_N* [46, 47]. These models do not include the QGP formation in the process of A+A collisions.
- **The QGP models** are as follows: Quark Combination (QuarkComb) model [48], 3-fluid dynamics (3FD) model [49–52], PHSD model [53–55] and Core-Corona model [56, 57]. These generators explicitly assume the QGP formation in A+A collisions.

Based on these assumptions the experimental data measured at the collision energies $\sqrt{s_{NN}} = 3.1, 3.6, 4.2, 4.9, 5.4, 6.3, 7.6, 8.8, 12.3$ and 17.3 GeV were analyzed in [12]. The collision energies $\sqrt{s_{NN}} \leq 4.9$ GeV correspond to Au+Au reactions studied at AGS. At $\sqrt{s_{NN}} = 5.4$ GeV the reactions Pb+Si, Si+Si and Si+Al were also investigated at AGS, while higher collision energies correspond to Pb+Pb reactions studied at SPS. Using the definitions (5) and (6) at each collision energy the available description of the transverse mass distributions, the longitudinal rapidity distributions and the hadronic yields measured at midrapidity or/and the total one obtained by a given model was arithmetically averaged for each kind of analyzed strange hadron. The QDDs and their errors obtained for each energy and for each hadron were arithmetically averaged over the models belonging to the same type. Then the QDDs and their errors found in this way for the models belonging to the same type were arithmetically averaged for each hadron and antihadron, if available, in order to reduce the number of data for a comparison. Finally, the resulting QDDs and their errors of the same same type of model were arithmetically averaged over all hadronic species. More details can be found in [12]. The

averaged QDDs of HG models $\langle \chi^2/n \rangle_{[h]}^{[A]}|_{HG}$ and the ones of QGP models $\langle \chi^2/n \rangle_{[h]}^{[A]}|_{QGP}$ were found in this way together with their errors. The results are shown in Fig. 3.

From Fig. 3 one can see that the meta-analysis of work [12] leads to an independent conclusion that the mixed phase exists at the same collision energy range $\sqrt{s_{NN}} = [4.3; 4.9]$ GeV which was originally found in [7, 8]. This result is important not only to validate the entire framework of shock adiabat model used in [7, 8], but also to justify the jump of the effective number of degrees of freedom s/T^3 at CFO and a sharp peak of the trace anomaly δ at CFO as reliable signals of QGP formation. In addition the meta-analysis of QDD [12] predicts that the most probable collision energy range of the second phase transition is $\sqrt{s_{NN}} = 10 - 13.5$ GeV. Thus, the meta-analysis of QDD supports an interpretation of the high energy set of correlated quasi-plateaus as an indicator of phase transition, although it shifts this transition to slightly higher collision energies.

Unfortunately, at present it is impossible to distinguish between two possible explanations of this phenomenon. The first possible explanation is that with increasing collision energy the initial states of thermally equilibrated matter formed in nucleus-nucleus collisions move first from the hadron gas into the mixed phase, then from the mixed phase to QGP and then again they return to the same mixed phase, but at higher initial temperature and lower baryonic density. Such a scenario corresponds to the case, if QCD phase diagram has a critical endpoint [12]. An alternative explanation [12] corresponds to the QCD phase diagram with the tricritical endpoint. In such a case the second phase transition is the second order phase transition of (partial) chiral symmetry restoration or a transition between quarkyonic matter and QGP [59]. It is necessary to stress, that despite the lack of a single interpretation of the second phase transition possibly existing at $\sqrt{s_{NN}} = 10 - 13.5$ GeV there are strong arguments [12] that the (tri)critical endpoint of QCD phase diagram maybe located at $\sqrt{s_{NN}} = 12 - 14$ GeV.

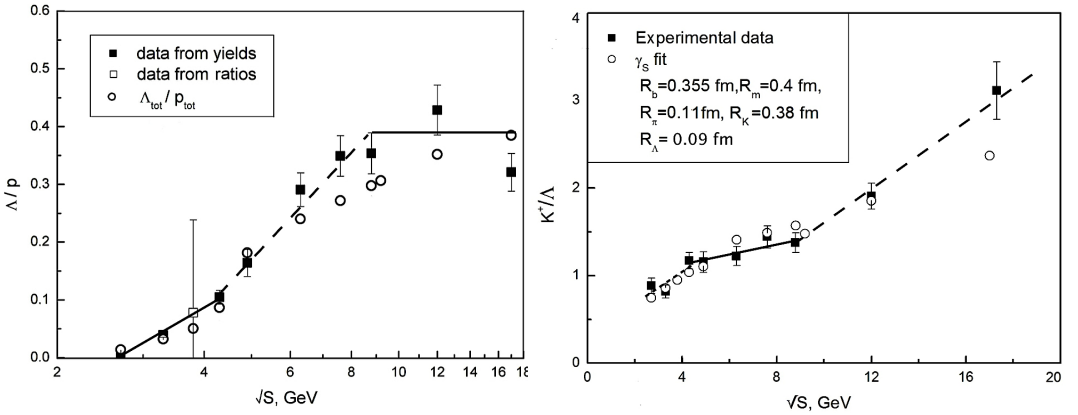


Figure 4. The collision energy dependence of the Λ/p (left) and K^+/Λ (right) ratios obtained within the present HRGM. The lines are given to guide the eye. More explanations are given in the text.

The combined conclusions obtained from inspecting two sets of correlated quasi-plateaus at CFO, two peaks of trace anomaly at CFO and the ones found out by the meta-analysis, led us a thorough analysis of the Λ/p and K^+/Λ ratios. From the left panel of Fig. 4 one can see that there are three regimes in the energy dependence of the Λ/p ratio: at $\sqrt{s_{NN}} = 4.3$ GeV the slope of this ratio clearly increases, while above $\sqrt{s_{NN}} = 8.8$ GeV it nearly saturates. The sudden increase of Λ/p slope at $\sqrt{s_{NN}} = 4.3$ GeV can be naturally explained by the idea of work [60] that the mixed phase formation

can be identified by a rapid increase in the number of strange quarks per light quarks. Evidently, the Λ/p ratio is a convenient indicator because at low collision energies Λ hyperons are generated in collisions of nucleons. Moreover, such a ratio does not depend on baryonic chemical potential, since both the protons and Λ hyperons have the same baryonic charge. As it is seen from the left panel of Fig. 4, this mechanism works up to $\sqrt{s_{NN}} = 4.3$ GeV, while an appearance of the mixed phase should lead to an increase of the number of strange quarks and antiquarks due to the annihilation of light quark-antiquark and gluon pairs. Clearly, this simple picture is well fitted into the prediction that the mixed phase can be reached at $\sqrt{s_{NN}} = 4.3$ GeV, while QGP is formed at $\sqrt{s_{NN}} \geq 4.9$ GeV. The dramatic decrease of the slope of the experimental Λ/p ratio at $\sqrt{s_{NN}} > 8.8$ GeV which is seen in Fig. 4 can be an evidence for the second phase transformation, which we discussed above.

It is appropriate to say a few words about the experimental data of hadron yields shown in both panels of Fig. 4. For the AGS collision energies $\sqrt{s_{NN}} = 2.7, 3.1$, and 4.3 GeV the yields of protons and kaons were, respectively, taken from Refs. [24] and [18], whereas for Λ -hyperons they were taken from Ref. [19]. Experimental yields measured at the highest AGS energy $\sqrt{s_{NN}} = 4.9$ GeV for protons and kaon were taken from Ref. [16, 24], while for Λ they were given in Ref. [23]. The mid-rapidity yields of protons, kaons and lambdas measured at the SPS energies $\sqrt{s_{NN}} = 6.3, 7.6, 8.8, 12$, and 17.3 GeV are provided by the NA49 collaboration in Refs. [26, 27, 29–31]. For a comparison, in Fig. 4 we also show the value with huge error bars which are found from other two ratios, Λ/π^- and p/π^- , for $\sqrt{s_{NN}} = 3.6$ GeV.

It is interesting that the energy dependence of the K^+/Λ ratio shows the change of slopes at the same energies as the Λ/p ratio. This can be seen from the right panel of Fig. 4. Note that in the dominant hadronic reactions the positive kaons and Λ hyperons are born simultaneously. Since both of these hadrons carry the strange charge, then the logic of work [60] is inapplicable to their ratio. Therefore, in contrast to an increase of the slope of the Λ/p ratio on the interval $\sqrt{s_{NN}} = [4.3; 8.8]$ GeV, the K^+/Λ ratio has a flattening of the slope on this collision energy interval. In the leading order this ratio is defined via the kaon mass m_K , the Λ mass m_Λ and two chemical potentials as $K^+/\Lambda \simeq \sqrt{\left[\frac{m_K}{m_\Lambda}\right]^3} \exp\left[\frac{m_\Lambda - m_K + 2\mu_S - \mu_B}{T}\right]$. Therefore, a small slope of this ratio at the interval $\sqrt{s_{NN}} = [4.3; 8.8]$ GeV evidences about the cancellation of energy dependencies of strange and baryonic chemical potentials, i.e. $m_\Lambda - m_K + 2\mu_S - \mu_B \simeq \text{Const}$ for $\sqrt{s_{NN}} = [4.3; 8.8]$ GeV. An increase of the K^+/Λ ratio at higher collision energies can be mainly explained by the fast decrease of the baryonic chemical potential.

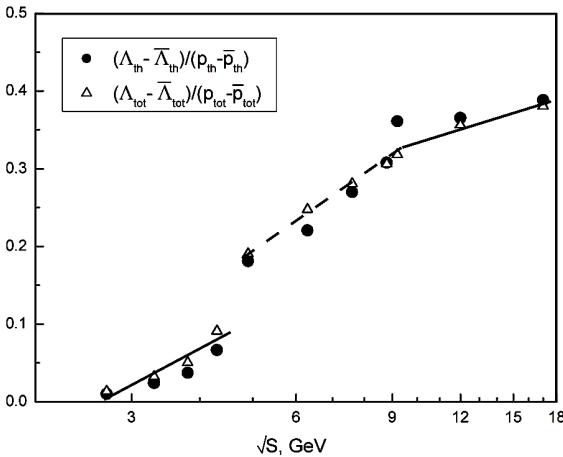


Figure 5. Most recent predictions for the collision energy dependence of the $\frac{\Delta\Lambda}{\Delta p}$ ratio. The triangles depict the ratio of total multiplicities, while the circles correspond to the ratio of thermal multiplicities. The lines are given to guide the eye.

Very recently a better description of the Λ/p ratio was achieved in [61], when more data were analyzed. Note that this result was obtained not on the expense of worsening of other hadron yield ratios. Based on this new fit of hadron yield ratios the predictions for the $\frac{\Delta\Lambda}{\Delta p} = \frac{\Lambda - \bar{\Lambda}}{p - \bar{p}}$ ratio are made. As one can see from Fig. 5 this ratio demonstrates even more dramatic changes in the collision energy dependence. Indeed, at the narrow collision energy interval $\sqrt{s_{NN}} = 4.3 - 4.9$ GeV this ratio has a strong jump, while at $\sqrt{s_{NN}} = 9.2$ GeV it shows a change of slope. Our educated guess is that the collision energy dependence of the $\frac{\Delta\Lambda}{\Delta p}$ ratio is an indicator of two phase transformations [61]. Since the observed jump of this ratio is located in the collision energy region of the mixed phase formation (i.e. with a first order phase transition), then a change of its slope at $\sqrt{s_{NN}} = 9.2$ GeV can be naturally associated with a weak first order or a second order phase transition. Note that such a hypothesis is well supported by the results of the meta-analysis [12] which is briefly summarized above.

4 Conclusions

From the discussions given in previous sections it is clear that a development of the multicomponent version of HRGM in 2012 led to a real breakthrough in our understanding of the thermodynamics at CFO. With the help of HRGM it was possible for the first time to describe the Strangeness Horn with the highest accuracy [3, 4, 6] including the topmost point. The new concept of separated CFOs for strange and non-strange hadrons with conservation laws connecting them allows one to naturally explain the appearance of apparent chemical non-equilibrium of strange particles [4]. Furthermore, a thorough analysis of the entropy per baryon and the pion number (thermal and total) per baryon at CFO led to a finding out of two sets of strongly correlated quasi-plateaus [7, 8]. Since the low energy set of quasi-plateaus was predicted in [9–11] as a signal of the quark-gluon-hadron mixed phase formation, then it was necessary to give a physical interpretation of the high energy set of quasi-plateaus.

A good hint to interpret the appearance of high energy set of quasi-plateaus is provided by the meta-analysis [12] of QDD. Since the QDD meta-analysis gave an independent evidence for the quark-gluon-hadron mixed phase formation at the narrow region of collision energy $\sqrt{s_{NN}} = 4.3 - 4.9$ GeV, then its predictions for the possible existence of another mixed phase at collision energies $\sqrt{s_{NN}} = 10 - 13.5$ GeV led us to a more thorough inspection of existing hadron multiplicity ratios. As one can see from the left panel of Fig. 4 the Λ/p ratio exhibits three different regimes in the collision energy dependence: at $\sqrt{s_{NN}} = 4.3$ GeV the slope of this ratio suddenly increases, while above $\sqrt{s_{NN}} = 8.8$ GeV it nearly saturates. As we argued above a strong increase of Λ/p slope at $\sqrt{s_{NN}} = 4.3$ GeV can be naturally explained by the idea of work [60] that the mixed phase formation can be identified by a rapid increase in the number of strange quarks per light quarks, while a dramatic decrease of the Λ/p slope at $\sqrt{s_{NN}} > 8.8$ GeV can be an evidence for the second phase transformation.

It is remarkable that the K^+/Λ ratio shows the change of slopes at the same energies as the Λ/p ratio, although the K^+/Λ ratio involves two strange particles and (in general) it strongly depends on the baryonic chemical potential. Also the trace anomaly at CFO shows two peaks at the collision energies $\sqrt{s_{NN}} = 4.9$ GeV and $\sqrt{s_{NN}} = 9.2$ GeV. The low energy trace anomaly peak can be explained within the shock adiabat model [8] as a signal of QGP formation, whereas the existence of high energy peak requires further confirmation by better experimental data. If it will be confirmed, then it will serve as a new indicator for a second phase transition. Nevertheless, already now all irregularities at CFO discussed here together with the results of the QDD meta-analysis form a coherent picture of possible observation of two mixed phases in nucleus-nucleus collisions. Therefore, the Beam Energy Scan program at RHIC has a unique chance to experimentally verify the above signals and to discover the mixed phases before the start of NICA and FAIR programs. The new observable, the $\frac{\Delta\Lambda}{\Delta p}$ ratio suggested in [61], will be very helpful for this because of its high sensitivity. However, to reach

such goals the RHIC experiments should provide much smaller error bars, especially at low energies. Hence, the experiments in a fixed target mode are absolutely necessary for the success of the Beam Energy Scan program at RHIC.

Acknowledgements

The authors are thankful to D. B. Blaschke, T. Galayuk, R. A. Lacey, I. N. Mishustin, D. H. Rischke, K. Redlich, L. M. Satarov, A.V. Taranenko, K. Urbanowski and Nu Xu for interesting discussions and valuable comments. K.A.B., A.I.I., V.V.S. and G.M.Z. acknowledge the partial support of the program “On perspective fundamental research in high-energy and nuclear physics” launched by the Section of Nuclear Physics of NAS of Ukraine. D.R.O. acknowledges a support of Deutsche Telekom Stiftung. K.A.B. is very thankful to all organizers of the ICNFP2015 for providing him with a chance to present and to discuss these results at the Conference and for a warm hospitality in OAC.

References

- [1] A. Andronic, P. Braun-Munzinger and J. Stachel, Nucl. Phys. A **772**, 167 (2006) and references therein.
- [2] D.R. Oliinychenko, K.A. Bugaev and A.S. Sorin, Ukr. J. Phys. **58**, 211 (2013).
- [3] K. A. Bugaev, D. R. Oliinychenko, A. S. Sorin, G. M. Zinovjev, Eur. Phys. J. A **49**, 30 (2013).
- [4] K. A. Bugaev *et al.*, Europhys. Lett. **104**, 22002 (2013).
- [5] V. V. Sagun, Ukr. J Phys. **59**, 755 (2014).
- [6] V. V. Sagun *et al.*, Ukr. J. Phys. **59**, 1043 (2014).
- [7] K. A. Bugaev *et al.*, Phys. Part. Nucl. Lett. **12**, 238 (2015).
- [8] K. A. Bugaev *et al.*, arXiv:1412.0718 [nucl-th] and references therein.
- [9] K. A. Bugaev, M. I. Gorenstein, B. Kämpfer and V. I. Zhdanov, Phys. Rev. D **40**, 2903 (1989).
- [10] K. A. Bugaev, M. I. Gorenstein and D. H. Rischke, JETP Lett. **52**, 1121 (1990).
- [11] K. A. Bugaev, M. I. Gorenstein and D. H. Rischke, Phys. Lett. B **255**, 18 (1991).
- [12] V. A. Kizka, V. S. Trubnikov, K. A. Bugaev and D. R. Oliinychenko, arXiv:1504.06483 [hep-ph].
- [13] J. Rafelski, Phys. Lett. B **62**, 333 (1991).
- [14] S. Wheaton, J. Cleymans and M. Hauer, Comput. Phys. Commun. **180**, 84 (2009).
- [15] J.L. Klay *et al.*, Phys. Rev. C **68**, 054905 (2003).
- [16] L. Ahle *et al.*, Phys. Lett. B **476**, 1 (2000).
- [17] L. Ahle *et al.*, Phys. Lett. B **490**, 53 (2000).
- [18] J.L. Klay *et al.*, Phys. Rev. Lett. **88**, 102301 (2002).
- [19] C. Pinkenburg *et al.*, Nucl. Phys. A **698**, 495 (2002).
- [20] J. Barrette *et al.*, Phys. Rev. C **62**, 024901 (2000).
- [21] L. Ahle *et al.*, Phys. Rev. C **60**, 064901 (1999).
- [22] L. Ahle *et al.*, Phys. Rev. C **58**, 3523 (1998).
- [23] S. Albergo *et al.*, Phys. Rev. Lett. **88**, 062301 (2002).
- [24] B. B. Back *et al.*, Phys. Rev. Lett. **87**, 1970 (2001).
- [25] I. G. Bearden *et al.*, Phys. Rev. C **66**, 044907 (2002).
- [26] S. V. Afanasiev *et al.*, Phys. Rev. C **66**, 054902 (2002).
- [27] S. V. Afanasiev *et al.*, Phys. Rev. C **69**, 024902 (2004).
- [28] C. Alt *et al.*, Phys. Lett. B **635**, 270 (2006).

- [29] T. Anticic *et al.*, Phys. Rev. Lett. **93**, 022302 (2004).
- [30] S. V. Afanasiev *et al.*, Phys. Lett. B **538**, 275 (2002).
- [31] C. Alt *et al.*, Phys. Rev. Lett. **94**, 192301 (2005).
- [32] F. Antinori *et al.*, Phys. Lett. B **595**, 65 (2004).
- [33] F. Antinori *et al.*, J. Phys. G **31**, 1345 (2005).
- [34] J. Adams *et al.*, Phys. Rev. Lett. **92**, 112301 (2004).
- [35] Sz. Borsanyi *et al.*, JHEP **1208**, 053 (2012).
- [36] K. A. Bugaev *et al.*, Ukr. J. Phys. **60**, 181 (2015).
- [37] P. Koch, B. Müller and J. Rafelski, Phys. Rep. **142**, 167 (1986) and references therein.
- [38] C. M. Hung and E. V. Shuryak, Phys. Rev. C **57**, 1891 (1998) and references therein.
- [39] Y. Pang, T. J. Schlagel and S.H. Kahana, Phys. Rev. Lett. **68**, 2743 (1992).
- [40] H. Sorge, Phys. Rev. C **52**, 3291 (1995).
- [41] W. Ehehalt and W. Cassing, Nucl. Phys. A **602**, 449 (1996).
- [42] W. Cassing and E. L. Bratkovskaya, Phys. Rep. **308**, 65 (1999).
- [43] J. Geiss, W. Cassing and C. Greiner, Nucl. Phys. A **644**, 107 (1998).
- [44] S. A. Bass *et al.*, Prog. Part. Nucl. Phys. **41**, 225 (1998).
- [45] F. Becattini, J. Manninen and M. Gazdzicki, Phys. Rev. C **73**, 044905 (2006).
- [46] R. Longacre, preprint BNL-48648, C93-01-13.
- [47] S. E. Eiseman *et al.*, Phys. Lett. B **297**, 44 (1992).
- [48] L. X. Sun, R. Q. Wang, J. Song and F. L. Shao, Chin. Phys. C **36**, 55 (2012).
- [49] Y. B. Ivanov, V. N. Russkikh and V. D. Toneev, Phys. Rev. C **73**, 044904 (2006).
- [50] Yu. B. Ivanov and V. N. Russkikh, Phys. Rev. C **78**, 064902 (2008).
- [51] Yu. B. Ivanov, Phys. Rev. C **87**, (2013) 064905.
- [52] Yu. B. Ivanov, Phys. Rev. C **89**, 024903 (2014).
- [53] W. Cassing and E. L. Bratkovskaya, Phys. Rev. C **78**, 034919 (2008).
- [54] W. Cassing, Eur. Phys. J. ST **168**, 3 (2009).
- [55] W. Cassing and E. L. Bratkovskaya, Nucl. Phys. A **831**, 215 (2009).
- [56] P. Bozek, Acta Phys. Pol. B **36**, 3071 (2005).
- [57] K. Werner, Phys. Rev. Lett. **98**, 152301 (2007).
- [58] J. R. Taylor, *An introduction to error analysis* (University Science Book, Mill Valley, California, 1982).
- [59] A. Andronic *et al.*, Nucl. Phys. A **837**, 65 (2010).
- [60] J. Rafelski and B. Müller, Phys. Rev. Lett. **48**, 1066 (1982).
- [61] K.A. Bugaev *et al.*, arXiv:1510.03099v1 [nucl-th] (2015).